CHRONIC CENTRAL ADMINISTRATION OF VALPROIC ACID: INCREASED PRO-SURVIVAL PHOSPHO-PROTEINS AND GROWTH CONE ASSOCIATED PROTEINS WITH NO BEHAVIORAL PATHOLOGY

by

RYAN CHRISTOPHER BATES

B.S., Metropolitan State University of Denver, 2006

A thesis submitted to the

Faculty of the Graduate School of the

University of Colorado in partial fulfillment

of the requirements for the degree of

Master of Science

Integrative Biology

2013

This thesis for the Master of Science degree by

Ryan Christopher Bates

has been approved for the

Integrative Biology Program

by

Bradley J. Stith, Chair

Jefferson Knight

Amanda Charlesworth

July 9, 2013

Bates, Ryan, Christopher. (M.S., Integrative Biology)

Chronic Central Administration of Valproic Acid: Increased Pro-Survival Phospho-Proteins and Growth Cone Associated Proteins with no Behavioral Pathology

Thesis Directed by Professor Bradley J. Stith

ABSTRACT

Valproic acid (VPA) is the most widely prescribed antiepileptic drug due to its ability to treat a broad spectrum of seizure types. However, potential complications of this drug include anticonvulsant polytherapy metabolism, organ toxicity and teratogenicity which limit its use in a variety of epilepsy patients. Direct delivery of VPA intracerebroventricularly (ICV) could circumvent the toxic effects normally seen with the oral route of administration. An additional potential benefit would be significantly reduced dosing while achieving high brain concentrations. Epileptogenic tissue from patients with intractable seizures has shown significant cell death which may be mitigated by maximizing cerebral VPA exposure. Here we show ICV administration of VPA localized to the periventricular zone increased pro-survival phospho-proteins ($pAkt^{Ser473}$, $pAkt^{Thr308}$, $pGSK3\beta^{Ser9}$, $pErk1/2^{Thr202/Tyr204}$) and growth cone associated proteins (2G13p, GAP43) in a whole animal system. No significant changes in DCX, NeuN, synaptotagmin, and synaptophysin were detected. Assessment of possible behavioral alterations in rats receiving chronic central infusions of VPA was performed with the open field and elevated plus mazes. Neither paradigm revealed any detrimental effects of the drug infusion process.

The form and content of this abstract are approved. I recommend its publication.

Approved: Bradley J. Stith

DEDICATION

I dedicate this thesis to my loving parents, Dale & Karen Bates, and to my "little" brother, Steven.

ACKNOWLEDGEMENT

I would like to thank Dr. Brad Stith and Dr. Doug Petcoff for their countless hours spent advising me about the complex world of bioscience and the games a scientist must play in order to win.

The contents of this thesis were published on August 31st 2012: Bates RC, Stith BJ, Stevens KE. Chronic central administration of valproic acid: increased pro-survival phospho-proteins and growth cone associated proteins with no behavioral pathology. *Pharmacology, Biochemistry and Behavior* 2012;103:237-244.

DOI Link: http://dx.doi.org/10.1016/j.pbb.2012.08.023

Paper featured on *Global Medical Discovery* with additional data figure (Fig. 4.) on March 19th 2013: http://globalmedicaldiscovery.com/key-scientific-articles/chronic-central-administration-of-valproic-acid-increased-pro-survival-phospho-proteins-and-growth-cone-associated-proteins-with-no-behavioral-pathology/

TABLE OF CONTENTS

CHAPTER

I. INTRODUCTION 1

II. MATERIALS AND METHODS 3

Animals 3

Implant Surgery 3

In Vivo Behavioral Studies 4

Tissue Preparations 5

Immunohistochemistry 5

Sample Lysate Preparation 6

Western Immunoblotting 7

Statistics 8

III. RESULTS 9

Behavior of ICV Implanted Rats in Open Field and Elevated Plus Maze……22

VPA, Phospho-Proteins, and Growth Cone Associated Protein Localization in Ventricle……28

Phospho-Protein and Total Protein Levels in Regional Brain Tissue Lysates..28

IV. DISCUSSION 18

V. CONCLUSION 24

REFERENCES 25

LIST OF FIGURES

FIGURE

1 Behavioral effects of ICV VPA administration 11

2 Immunochemical results of ICV VPA administration 14

3 Growth cone-associated proteins after ICV VPA administration 16

4 Drug penetrance and cases of hydrocephaly 17

LIST OF TABLES

TABLE

1 ANOVA results for Open Field and Elevated Plus Paradigms..... 10

2 ANOVA and Scheffe *a posteriori* results for Immunohistochemistry and Western blot studies 12

LIST OF ABBREVIATIONS

Erk, extracellular signal-regulated kinase

GSK3β, glycogen synthase kinase 3 beta

GAP43, growth associated protein 43

ICV, intracerebroventricle

VPA, valproic acid

CSF, cerebrospinal fluid

BBB, blood brain barrier

EP, elevated plus maze

OF, open field maze

SUDEP, sudden unexpected death in epilepsy

DCX, doublecortin

NeuN, neuronal nuclei

CC, corpus callosum

LV, lateral ventricle

TV, third ventricle

H, hippocampus

CHAPTER I

INTRODUCTION

Mortality in epilepsy patients, specifically the occurrence of sudden unexpected death (SUDEP), is 24-40 times higher than those of the general population (Hitiris et al., 2007; Nobili et al., 2010) and seems to preferentially affect those with chronic intractable epilepsy (Asadi-Pooya and Sperling, 2009). Other negative outcomes are seen in chronic childhood epilepsy which is suggested to increase the likelihood of mental retardation and severely perturbed brain development (Choi et al., 2009; Wasterlain and Shirasaka, 1994). Brain tissue removed from patients with chronic intractable seizures displayed significant cell death among both neurons and astrocytes that was increased by seizure frequency (Choi et al., 2009). Surgical resection of an epileptogenic zone is usually performed in a large portion of temporal lobe epilepsy patients who are refractory to pharmacological intervention at a tolerable antiepileptic dose range (Vreugdenhil et al., 1998). Resection is generally followed by initiation of treatment with one of the most effective antiepileptic drugs, valproic acid (VPA) (Vreugdenhil et al., 1998), a drug shown to be effective in a significant proportion of treatment-resistant patients who did not undergo surgical resection (Chayasirisobhon and Russell, 1983; Gal et al., 1988; Hassan et al., 1976; Redenbaugh et al., 1980).

VPA's ability to help manage seizures is thought to be attributed to its multifaceted capability in affecting several targets. In rats, peripherally administered VPA increased the inhibitory neurotransmitter, γ-aminobutyric acid (GABA) (Godin et al., 1969; Higuchi et al., 1986; Loscher, 1981, 1999), and within the timeframe of increasing GABA, rodents were found to have decreased susceptibility towards seizures

(Loscher, 1981; Schechter et al., 1978; Simler et al., 1973). Others report that VPA modulated voltage-gated sodium channels (Cunningham et al., 2003; Vreugdenhil et al., 1998), calcium influx buffering during events of glutamate-induced toxicity (Zhang et al., 2010) and lowered aspartate release (Loscher, 1999). Additionally, VPA exposure to neuron and glial cell cultures has shown increases in the pro-cellular-survival phospho-proteins, $pAkt^{Ser473}$, $pAkt^{Thr308}$, $pGSK3\beta^{Ser9}$and $pErk1/2^{Thr202/Tyr204}$ (Di Daniel et al., 2005; Lamarre and Desrosiers, 2008; Pan et al., 2005). While there are numerous benefits to the peripheral administration of VPA to patients, side effects such as hyperammonemia (DeWolfe et al., 2009) and a reduction in drug clearance (Faught et al., 1999) can lead to complications endangering or further lowering quality of life.

In the present study, we record differential phospho-protein and growth cone associated protein levels in brain tissue with ICV administration of VPA in a whole animal model. VPA deposition was visualized at the drug release site to help understand penetrance within the central infusion context. Behavioral paradigms were also run to help determine if there was any onset of overt route-specific behavioral perturbations during the chronic exposure.

CHAPTER II

MATERIALS AND METHODS

Animals

Adult male Sprague Dawley rats (Harlan™ Sprague-Dawley; Indianapolis, IN) were housed in pairs prior to experiments under constant temperature (21 ±1 C) and 12-hour lighting (lights on from 6 a.m. to 6 p.m.). Rats were given access to water and rodent chow (Harlan Teklad, Indianapolis, IN) *ad libitum*. Procedures were approved by the Institutional Animal Care and Use Committee (IACUC, Veterans Affairs Medical Center, Eastern Colorado Healthcare System) and followed American Association for Laboratory Animal Science (AALAS) guidelines.

Implant Surgery

Rats (250-280 g) were administered atropine sulfate (0.4 mg/kg, ip) as a preanesthetic 10 minutes prior to an injection of sodium pentobarbital (60 mg/kg, ip, Nembutal®, Hospira, Inc.; Lake Forest, IL). They were stereotaxically implanted with a cannula (Brain Infusion Kit 1, ALZET®, Durect, Cupertino, CA) aimed at one anterior lateral ventricle [-1 mm posterior to bregma; -1.2 mm lateral to midline and; 4.0 mm ventral to skull (Paxinos and Watson, 1997)]. The cannula was attached by tubing to an osmotic minipump (0.25 μl/hr for 28 days, ALZET®, Durect, Cupertino, CA) loaded with saline, or valproic acid (pH 7.4) 2 or 3 mM . Great care was taken to guarantee no air bubbles were trapped in tubing (slow backfilling), our experience with this suggests that trapped air does affect pump rate. The cannula was secured to the skull with stainless steel screws and acrylic cement. The osmotic minipump was inserted into a subcutaneous pocket at shoulder level and the wound was closed with wound clips. A

prophylactic injection of enrofloxacin (20 mg/kg; Baytril®; BAYER HealthCare Inc.; Leverkusen, Germany) was administered at the end of the surgical procedure.

In Vivo Behavioral Studies

Implanted rats were allowed to recover for 14 days prior to behavioral testing. Behavioral testing was performed in a counterbalanced design to eliminate any potential order-of-testing effects. On the 15th day, half of the rats in each group were tested in the elevated plus (EP) maze (Carobrez and Bertoglio, 2005; Cruz et al., 1994; Doremus et al., 2006; Pellow et al., 1985), while the other half was tested in the open field (OF) maze (Ennaceur et al., 2006a, 2006b; Lipkind et al., 2004; Prut and Belzung, 2003; Stanford, 2007). On day 22, the groups were reversed.

For the EP maze, a rat was placed in the open region of a black Plexiglas '+' shaped platform with 13 cm wide arms. Two of the arms were enclosed by 32 cm high walls while the remaining 2 arms were open. The maze was elevated 51 cm off the floor. Rat movements were computer tracked for 5 min; the percent time spent in each type of arm and distance traveled in each arm (open, closed or in the center square) were computer analyzed (TopScan; Clever Sys Inc.; Reston, VA).

The open field consisted of a 104×104 cm^2 black Plexiglas floor with 39 cm high walls. The rat was placed near one side wall of the field and allowed to explore at will for 5 min during which its activity was computer monitored (TopScan; Clever Sys Inc.; Reston, VA). The field was divided into 3 regions (3 concentric squares), the outer region (adjacent to the walls), a middle region and the center square. Time and distance of travel in each region were computer calculated.

Tissue Preparations

A separate group of implanted rats was anesthetized with isoflurane inhalant anesthesia (3% in oxygen; Webster Veterinary; Sterling, MA) and perfused transcardially with a solution of 0.9% NaCl for 5 minutes followed by buffered 10% formaldehyde (Fisher Diagnostics; 23-245-685; Kalamazoo, MI) for 15 minutes. Brains were then excised and postfixed in the same fixative for 2 days. 1 mm coronal sections through the whole brain were cut using a sectioning block (Alto, 1 mm; BS-6000C; Braintree Scientific, Inc.; Braintree, MA).

Immunohistochemistry

Rat brain sections were incubated in undiluted blocking buffer (LI-COR® Biosciences; 927-40000; Lincoln, NE) for 2 hours on a rotator (Stovall; The Belly Dancer Lab Shaker) at room temperature. The fixed tissue sections were then incubated with primary antibodies in undiluted blocking buffer for 12 hours at 4-8°C. The specific antibodies employed in this study were: valproic acid pAb (rabbit; 1:1000; Abcam®; ab37127; Cambridge, MA), GSK3β^{Ser9} mAb (rabbit; 1:1000; Cell Signaling Technology®; 9323; Boston, MA), 2G13 mAb (mouse; 1:200; Novus Biologicals®; NB600-785; Littleton, CO), and AKT^{Ser473} mAb (rabbit; 1:1000; Cell Signaling Technology®; 4060; Boston, MA). Tissue slices were never allowed to dry; antibody incubations were unobstructed to prevent unequal tissue exposure (e.g. edge effect) in control and treated samples (True, 2008). Following two quick washes and two 30 minute washes, each with TBS containing 0.05% Tween-20 (TBST), the tissue sections were incubated for 2.5 hours at room temperature with IRDye® 800CW goat anti-rabbit pAb antibody (1:5000; LI-COR® Biosciences; 926-32211; Lincoln, NE) or IRDye®

680LT goat anti-mouse pAb antibody (1:5000; LI-COR® Biosciences; 926-68020; Lincoln, NE). The tissue sections received two quick washes and then two 1.5 hour washes in TBST. After washing, the tissue slices were placed in PBS buffer (pH 7.4) until arranged on the Odyssey® glass bed (LI-COR® Biosciences; Odyssey® Infrared Imager System; Lincoln, NE). PBS was applied to slices and a silicone mat placed on top for equal laser strike between individual slices. Fluorescent immunocomplexes around the periventricular zone were detected with the LI-COR® Odyssey® (700 nm and/or 800 nm channel, 21 μm resolution, and highest quality); intensity of the cannula path was not included in data collection. Laser intensity was optimized for each sample group. Typical laser intensity settings ranged from 2.0 to 4.0 for VPA exposed samples. Control samples were hit with a higher intensity, 4.5-5.5, so the ventricles could be visualized for figure images. Integrated intensities were determined with the Odyssey® system software (v 2.1).

Sample Lysate Preparation

A third group of implanted rats were anesthetized, perfuse-fixed, and decapitated as described above. Brain tissue was removed, and 1 mm coronal sections were cut on a sectioning block as above, starting from the cannula insertion point and moving both anteriorly and posteriorly. The first two 1 mm sections from the insertion point were removed (anterior section/posterior section) and periventricular tissue regions collected. Dissected regions were placed in microfuge tubes with 50 μl of 2% SDS, 200 mM DTT, 20 mM Tris-HCl (pH 7), phosphatase inhibitors (Sigma-Aldrich; P2850; P5726; St. Louis, MO), Protease Arrest™ (Cambiochem/EMD; 539124; Gibbstown, NJ) heated at 100^{o} C for 20 minutes then lowered to 80^{o} C for 2 hours (Addis et al., 2009; Becker et al.,

2008; Faratian et al., 2011; Shi et al., 2006). Lithium dodecyl sulfate (LDS) buffer (Invitrogen; NP0008; Carlsbad, California) was added to samples, vortexed, and stored at -20 C until used in Western blot studies.

Western Immunoblotting

Samples were thawed at room temperature and loaded into an electrophoresis chamber (Invitrogen, Midi-Cell Runner WR0100, Carlsbad, California) with NuPAGE® Novex 4-12% Bis-Tris Midi gels (Invitrogen, WG1403 Carlsbad, California) and transferred (Invitrogen, Novex Semi-Dry Blotter SD1000 Carlsbad, California) to a PDVF membrane (Millipore, Immobilon-FL IPFL07810 Billerica, MA). The membrane was then incubated in undiluted blocking buffer (LI-COR® Biosciences; 927-40000; Lincoln, NE) for 1 hour on a rotator (Stovall; The Belly Dancer Lab Shaker) at room temperature. Antibodies were added to undiluted blocking buffer and poured over the blot, then allowed to rotate for 1 hour. The specific antibodies employed in this study were: GSK3β mAb (rabbit; 1:1000; Cell Signaling Technology®; 9315; Boston, MA), GAPDH mAb (mouse; 1:1000; Novus Biologicals®; NB300-221; Littleton, CO), GAP43 pAb (rabbit; 1:1000; Cell Signaling Technology®; 5307; Boston, MA), NeuN mAb (mouse; 1:1000; Millipore®; MAB377; Billerica, MA), Doublecortin pAb (rabbit; 1:1000; Cell Signaling Technology®; 4604; Boston, MA), Synaptotagmin 1 (SYT1) pAb (rabbit; 1:1000; Cell Signaling Technology®; 3347; Boston, MA), Synaptophysin mAb (rabbit; 1:1000; Cell Signaling Technology®; 5461; Boston, MA), AKT mAb (rabbit; 1:1000; Cell Signaling Technology®; 2938; Boston, MA), p44/42 MAPK (Erk1/2) mAb (rabbit; 1:1000; Cell Signaling Technology®; 4695; Boston, MA), GSK3β^{Ser9} mAb (rabbit; 1:1000; Cell Signaling Technology®; 9323; Boston, MA), p44/42 MAPK

(Erk1/2)$^{Thr202/Tyr204}$ mAb (rabbit; 1:1000; Cell Signaling Technology®; 4370; Boston, MA), AKT^{Ser473} mAb (rabbit; 1:1000; Cell Signaling Technology®; 4060; Boston, MA), AKT^{Thr308} mAb (rabbit; 1:1000; Cell Signaling Technology®; 2965; Boston, MA). Following two quick washes and one 20-minute wash, each with TBS containing 0.05% Tween-20 (TBST), the blot was then incubated for 1 hour at room temperature with IRDye® 800CW goat anti-rabbit pAb antibody (1:10,000; LI-COR® Biosciences; 926-32211; Lincoln, NE) and/or IRDye® 680LT goat anti-mouse pAb antibody (1:20,000; LI-COR® Biosciences; 926-68020; Lincoln, NE). The blot again received two quick washes and then one 20-minute wash in TBST. After washing, it was placed in cold PBS buffer (pH 7.4) until arranged on the Odyssey® glass bed (LI-COR® Biosciences; Odyssey® Infrared Imager System; Lincoln, NE). A silicone mat was placed on top for equal laser strike between locations. Fluorescent immunocomplexes were detected with the LI-COR® Odyssey® (700 nm and/or 800 nm channel, 84 μm resolution, and highest quality). Channel sensitivity was optimized for each blot. Typical laser intensity settings ranged from 3.0 to 6.0 and integrated intensities were determined with the Odyssey® system software. The GAPDH intensity of each sample was used for normalization.

Statistics

One-way analysis of variance (ANOVA), with Scheffe multiple comparison *a posteriori analyses* where appropriate, were performed using SSPS version 19 for Windows (IBM; Somers, NY). All graphs were made using SigmaPlot 12 (Systat Software; San Jose, CA).

CHAPTER III

RESULTS

Behavior of ICV Implanted Rats in Open Field and Elevated Plus Maze

Rats with chronic administration of either saline or VPA (2 or 3 mM) were tested in both the OF and EP mazes to determine if there were any significant behavioral alterations produced by the intervention (*n*=8 each group; individual animals). Testing began after 14 days of post-surgery to allow for any potential VPA toxicity to elicit effects before collecting data. ANOVA for the OF/EP studies, assessing percent time spent in specific regions or arms and total distance traveled, showed no significant changes (Fig. 1.; Table 1). These data demonstrate that chronic central administration of valproic acid did not produce any detrimental behavioral effects in these rats.

Table 1
ANOVA results for Open Field and Elevated Plus Paradigms

Paradigm	**Variable**	**Region**	**$F_{(2,21)}$**	***p***
Open field	*Percent time in region*	Outer	0.754	0.483
		Middle	0.783	0.470
		Center	1.000	0.385
	Distance traveled in region	Outer	0.197	0.822
		Middle	0.538	0.592
		Center	1.000	0.385
	Percent time in arm			
Elevated plus		Closed	0.836	0.447
		Open	0.708	0.504
	Distance traveled in arm	Center	0.318	0.731
		Closed	0.408	0.670
		Open	0.090	0.914
		Center	0.004	0.996

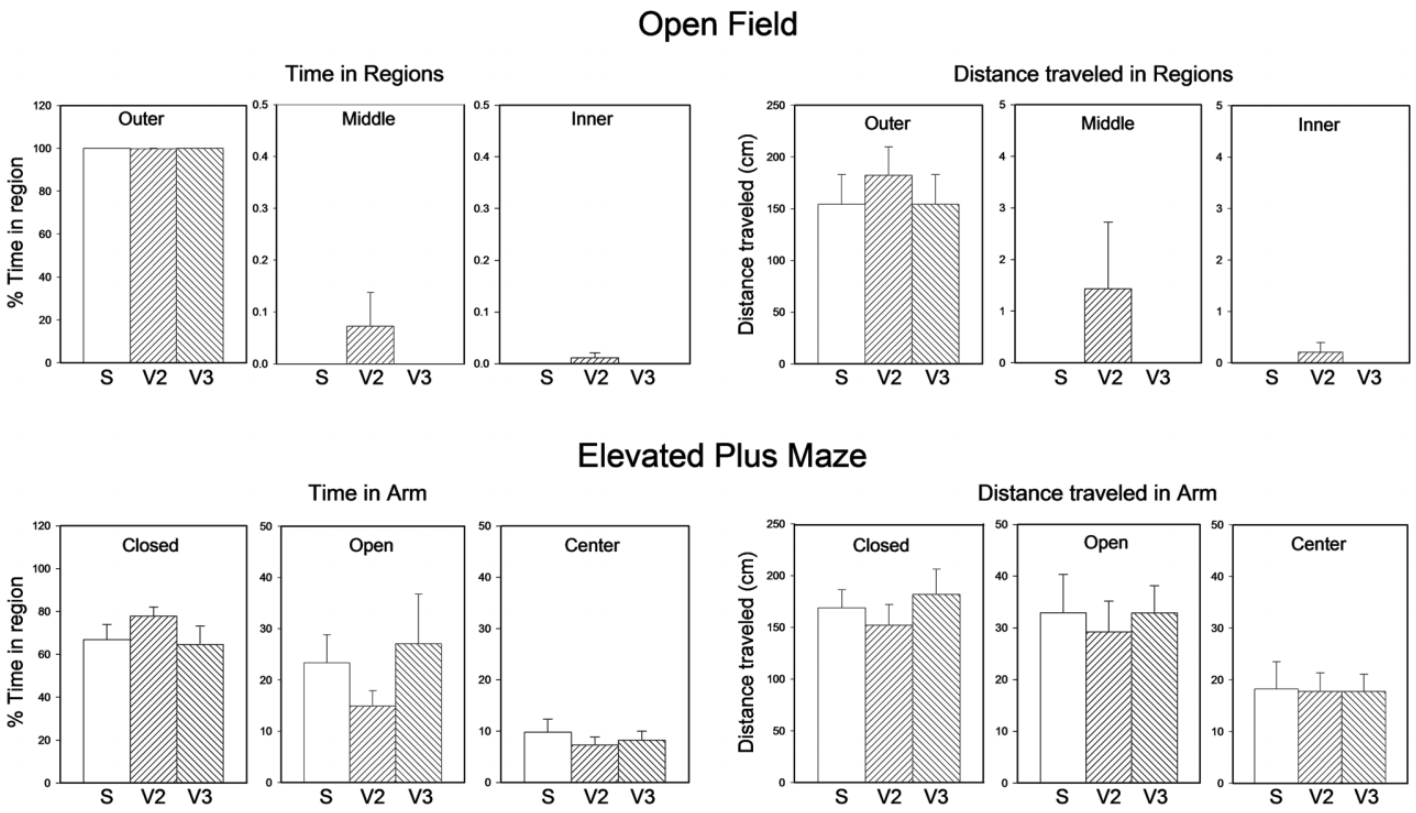

Figure 1 Behavioral effects of ICV VPA administration. Male Sprague Dawley rats were implanted with an osmotic minipump delivering saline (S), 2 mM (V2) or 3 mM (V3) valproic acid directly into the right lateral ventricle. In the open field and elevated plus maze, there were no significant differences observed in distance traveled over the 5 minutes of testing, suggesting that VPA did not cause sedation in these animals, nor was there any significant effect on anxiety. Data are mean ± SEM; *n*=8; individual animals.

Table 2
ANOVA and Scheffe *a posteriori* results for Immunohistochemistry and Western blot studies

Figure	Region sample	$F_{(2,15)}$	Saline vs. 2 mM VPA *p*	Saline vs. 3 mM VPA *p*	2 mM vs. 3 mM VPA *p*
Fig.2.A. Valproic acid	*Right vent*	43.38	<0.001*	<0.001*	0.773
Fig.2.B. $pAkt^{Ser473}$	*Right vent*	62.70	<0.001*	<0.001*	*0.391*
Fig.2.C. $pGSK3\beta^{Ser9}$	*Right vent*	200	<0.001*	<0.001*	0.004*
Fig.2.D $pAkt^{Ser473}$	Top right	117	<0.001*	<0.001*	0.616
	Right vent	19.26	<0.001*	0.001*	0.532
	Left vent	23.56	<0.001*	<0.001*	0.878
Fig.2.E. $pAkt^{Thr308}$	Top right	13.18	0.006*	0.001*	0.597
	Right vent	22.30	<0.001*	0.001*	0.231
	Left vent	10.38	0.002*	0.024*	0.434
Fig.2.F. pErk1/2 $^{Thr202/Tyr204}$	Top right	65.59	<0.001*	<0.001*	0.005*
	Right vent	7.72	0.024*	0.009*	0.865
	Left vent	4.57	0.105	0.039*	0.855
Fig.2.G. $pGSK3\beta^{Ser9}$	Top right	37.57	<0.001*	<0.001*	0.886
	Right vent	36.25	<0.001*	<0.001*	0.623
	Left vent	59.89	<0.001*	<0.001*	0.081
Fig.3.A. 2G13	*Right vent*	45.50^{A}	<0.001*	<0.001*	0.006*
Fig.3.B. GAP43	Top right	102	<0.001*	<0.001*	0.048*
	Right vent	44.59	<0.001*	<0.001*	0.130
	Left vent	69.72	<0.001*	<0.001*	0.511
Fig.3.B. Synaptophysin	Top right	0.385	0.865	0.692	0.948
	Right vent	0.497	0.981	0.649	0.759
	Left vent	0.532	0.537	0.908	0.788
Fig.3.B. Synaptotagmin	Top right	0.224	0.802	0.940	0.951
	Right vent	0.360	0.836	0.720	0.977
	Left vent	0.285	0.762	0.967	0.890

Table 2 (con't)

Fig.3.B. Doublecortin (DCX)	Top right	0.318	0.752	0.844	0.984
	Right vent	0.397	0.679	0.909	0.903
	Left vent	0.242	0.993	0.868	0.811
Fig.3.B. NeuN	Top right	0.166	0.858	0.921	0.989
	Right vent	0.421	0.925	0.665	0.875
	Left vent	0.710	0.516	0.760	0.913

[A]$F_{(2,33)}$: Due to the method, antibody multiplexing was possible and allowed for increased sample collection of this protein. (*$p<0.05$)

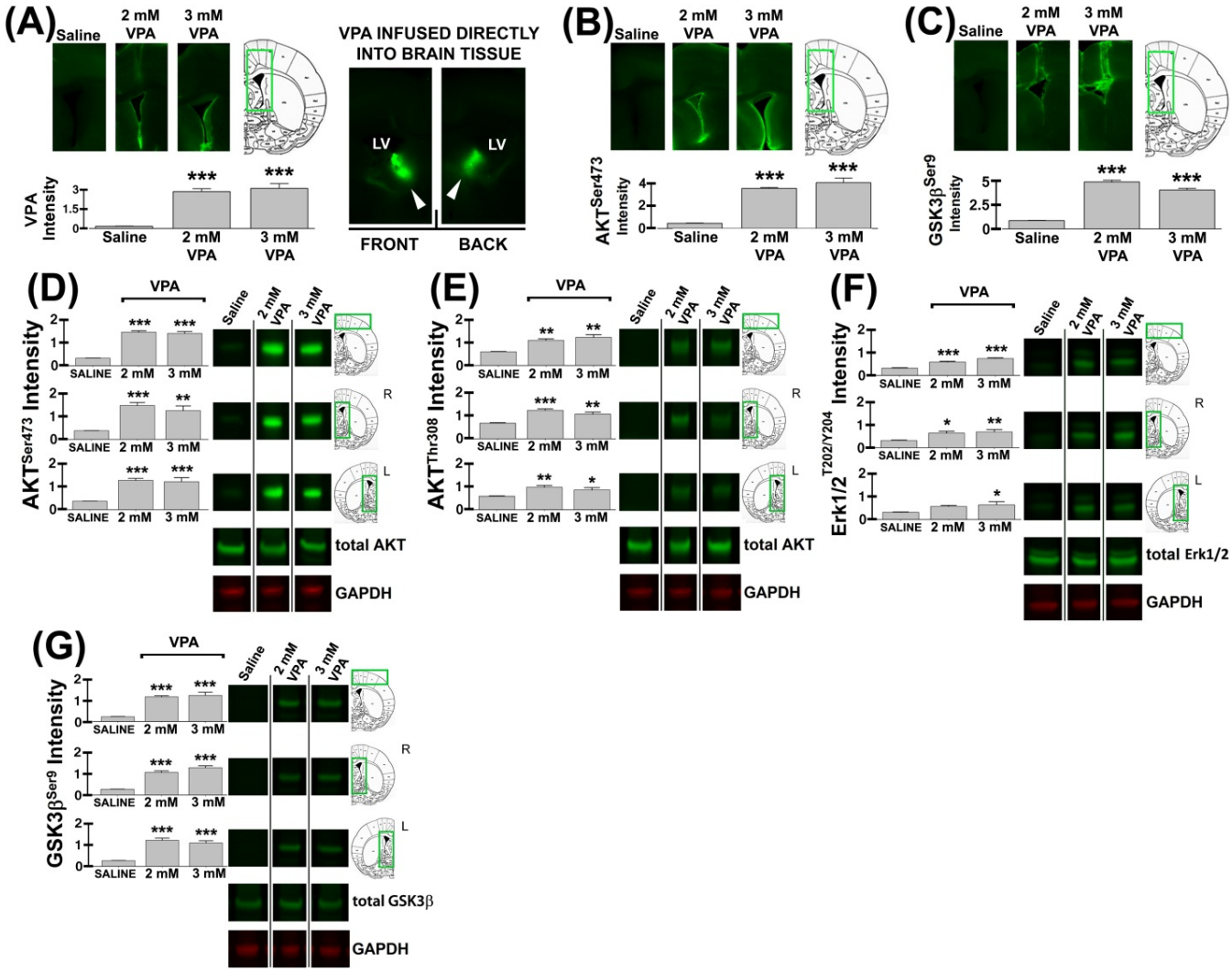

Figure 2 Immunochemical results of ICV VPA administration. Results of immunohistochemistry showing valproic acid, released intracerebroventricularly (ICV) for 28 days, localized primarily to the periventricular zone (A). Verifying VPA antibody specificity was done by terminating the cannula end directly into brain tissue, adjacent to the lateral ventricle (LV) (A). Increases in phosphoprotein presence were also detected in tissue slices of this region (B, C). Infrared Western blotting results of VPA-exposed brain regions showed increases in pro-survival protein phosphorylation states (D, E, F, G)

when compared to saline controls. Data are mean ± SEM; *n*=6; individual animals (*p<0.05, **p<0.01, ***p<0.001).

VPA, Phospho-Proteins, and Growth Cone Associated Protein Localization in Ventricle

Fixed brain slices from rats treated with VPA showed a significant immunopositive presence for the drug itself versus saline control (Fig. 2. A.; Table 2; *n*=6; individual animals). With placement of the cannula within the ventricular space, penetrance of VPA appeared to primarily localize in the periventricular zone and cannula tract. An increase in 2G13p, a protein associated with axon growth cone formation, was detected in this same area (Fig. 3. A.; Table 2; *n*=12; individual animals) along with $pAkt^{Ser473}$ and $pGSK3\beta^{Ser9}$ (Fig. 2. B, C.; Table 2; *n*=6; individual animals).

Phospho-Protein and Total Protein Levels in Regional Brain Tissue Lysates

Pro-survival phospho-proteins were assayed for in dissected tissue locations using infrared Western blot analysis. In rats with central administration of VPA there were significant increases in $pAkt^{Ser473}$, $pAkt^{Ser308}$ and $pGSK3\beta^{Ser9}$ (Fig. 2. D, E, F.; Table 2; *n*=6; individual animals). $pErk1/2^{Thr202/Tyr204}$ had significant increases, except in saline vs. 2 mM (left vent) (Fig. 2. G.; Table 2; *n*=6; individual animals). GAP43, another growth cone associated protein, showed significant increases in saline vs. 2 mM/3 mM VPA within all three regions (Fig. 3. B.; Table 2; *n*=6; individual animals). Synaptophysin, synaptotagmin, NeuN and doublecortin (DCX) all had non-significant changes in the selected areas during exposure to valproic acid (Fig. 3. B.; Table 2; *n*=6; individual animals).

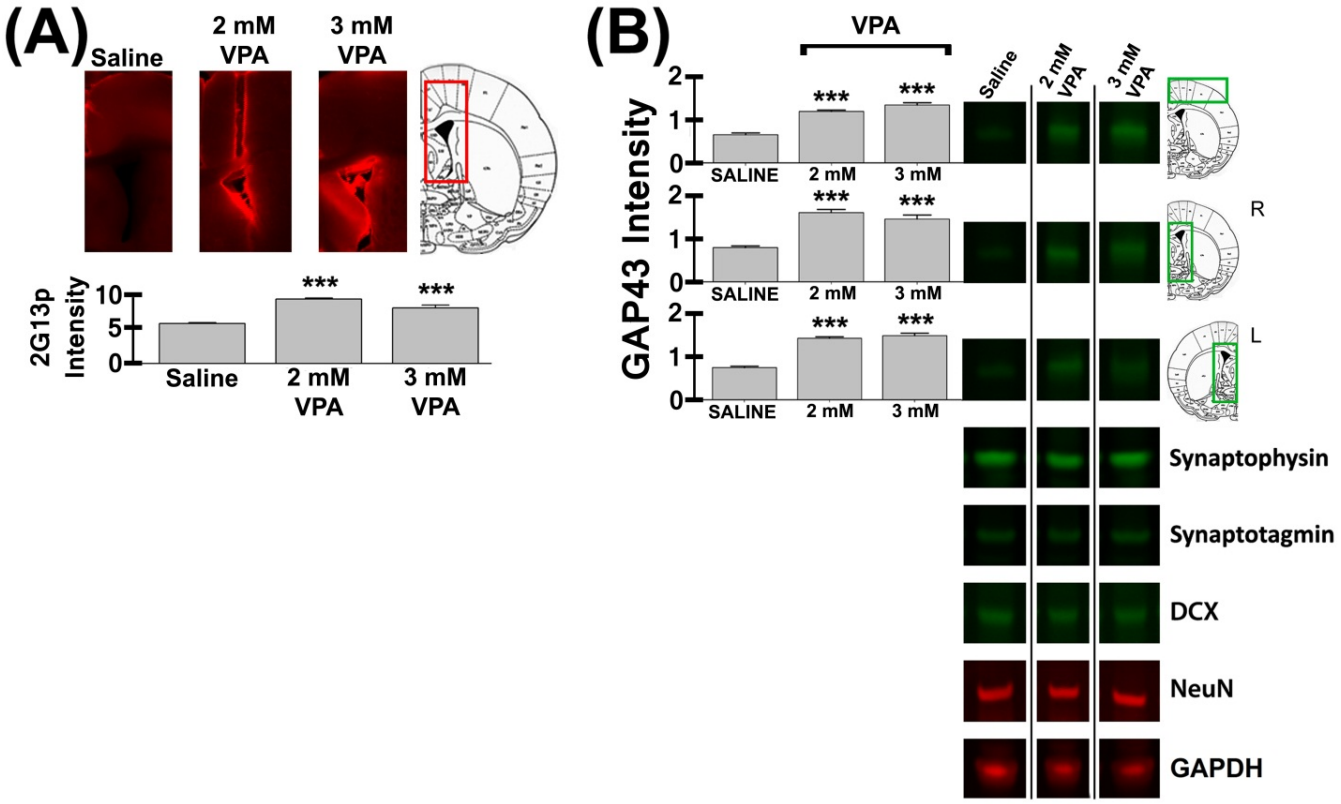

Figure 3 Growth cone-associated proteins after ICV VPA administration. Tissue sections and immunoblots show increased presence of growth cone associated proteins, 2G13p and GAP43, after chronic ICV infusion of valproic acid (A, B). Results, however, did not display any significant change in proteins associated with synaptic vesicle populations or mature/immature neurons (B). Data are mean ± SEM; (A) *n*=12; individual animals, (B) *n*=6; individual animals (*p<0.05, **p<0.01, ***p<0.001).

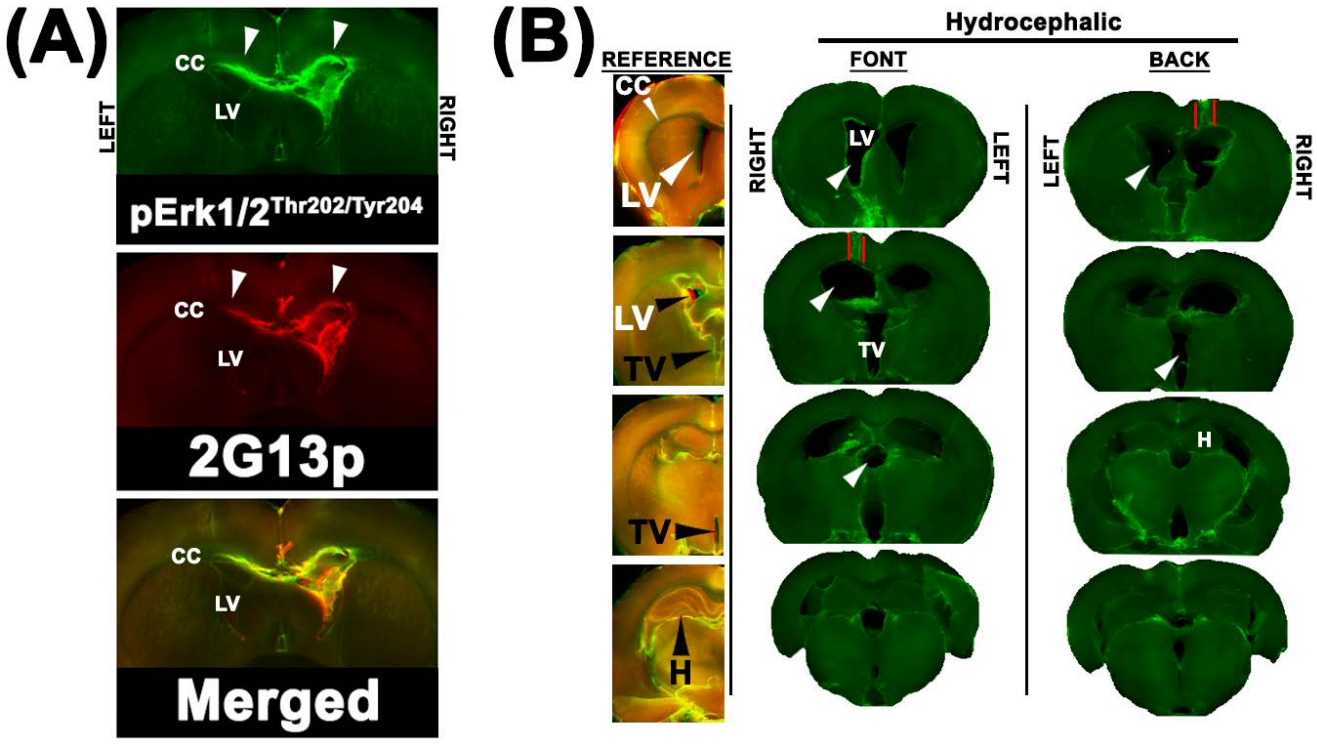

Figure 4 Drug penetrance and cases of hydrocephaly. Fig. A. While testing cannula termination sites for VPA drug release, implantation into the corpus callosum displayed expanding increases of pErk1/2$^{Thr202/Tyr204}$ and the growth cone protein (2G13p) within CC tissue (infused 28 days; 2 mM). Immunocomplexes for the two targets significantly increased as expected in the right CC release site, but also had expanded into the left hemisphere, suggested primarily through CC tissue. Fig. B. Several rats that were centrally administered 3 mM VPA within the right lateral ventricle (LV) displayed significant hydrocephaly. Arrows indicate some areas with markedly widened ventricles and the cannula insertion point is indicated between red lines. Abbreviations: VPA, valproic acid; CC, corpus callosum; LV, lateral ventricle; TV, third ventricle; H, hippocampus.

CHAPTER IV

DISCUSSION

The lack of behavioral changes in the EP/OF paradigms suggests that, at least at the doses tested and for the two behavioral tests performed, continuous central administration of VPA has no overt behavioral effects on anxiety nor was there evidence of sedation or behavioral activation. These studies stand in contrast to work by Serralta and colleagues (Serralta et al., 2006) where central injections of VPA produced significant ataxia and sedation, albeit the concentrations used in present studies were significantly lower than the Serralta study (288-432 μg/ml versus 400 mg/ml). While the present study did not assess seizure reduction with continuous central VPA administration, the Serralta study has shown significant reduction in seizure intensity, duration and after discharge duration with continuous ICV administration of VPA using the kindled rat model (Serralta et al., 2006), again with the caveat of significantly lower concentrations in the present studies. In contrast to the lack of behavioral effects, there were significant changes observed with a number of biochemical markers. Tissue penetration of VPA, following chronic ICV release was localized primarily along the periventricular zone and the cannula track where there were increases in pro-survival $pAkt^{Ser473}$, $pGSK3\beta^{Ser9}$ and growth cone 2G13p. In addition, analysis of the lysates of the three dissected regions of VPA treated rats showed elevated levels of pro-survival $pAkt^{Ser473}$, $pAkt^{Thr308}$, $pGSK3\beta^{Ser9}$, $pErk1/2^{Thr202/Tyr204}$, and growth cone GAP43, while there were no significant changes in DCX, NeuN, synaptotagmin, and synaptophysin. These findings suggest that delivery of VPA directly into the lateral ventricle promotes a pro-survival and pro-growth cone signaling environment in the periventricular region.

These profiles are present in tissue surrounding the ventricular space which contains the cannula termination point and extend to other contiguous areas of cerebrospinal fluid (e.g. left ventricular space). Specific behavior, synaptic vesicle proteins, and neuron maturation markers appear to not be affected by the VPA infusion process. Low tissue penetrance may occur, which could limit drug efficacy and may explain the failed trials for Parkinson's disease (Nutt et al., 2003; Salvatore et al., 2006).

VPA has been shown to elevate $pAkt^{Ser473}$ in neural SH-SY5Y cells (Pan et al., 2005) and $pAkt^{Thr308}$ in glial U-87 cells (Lamarre and Desrosiers, 2008). The present study sought to determine if central administration of VPA would produce effects similar to those seen in the blastoma cell lines. Since phosphorylation of Thr308 and Ser473 are both required for complete activation of Akt (Datta et al., 1999; Kandel and Hay, 1999; Scheid and Woodgett, 2001), our data suggests that the fully activated form is present when whole brain tissue is exposed to VPA. Other reports have shown variable conditions leading to differential Akt phosphoprotein states (Khor et al., 2004; Kitagawa et al., 2002; Kumari et al., 2001; Obara et al., 2002; Ouyang et al., 2000; Velling et al., 2008) along with downstream pro-survival effects. This suggests that both Akt sites are not needed for survival (Datta et al., 1999; Kandel and Hay, 1999; Scheid and Woodgett, 2001) and supports our measurement of both phosphorylation sites. An example of phospho-specific activity is reported by Goren et al (2008), who showed that phosphorylation at Thr308 of Akt1 allows for exclusion from the nucleus with insulin exposure in keratinocytes. Akt should induce an increase in the inhibitory phospho-form, $GSK3\beta^{Ser9}$ (Chin et al., 2005; Cross et al., 1995; Grimes and Jope, 2001), and our results are in agreement with this effect.

Consistent with our results, oral administration of VPA in rats has been shown to increase pErk1/2$^{Thr202/Tyr204}$ (Einat et al., 2003) which is also seen with exogenous exposure in SH-SY5Y cells and rat primary cortical neurons (Di Daniel et al., 2005). The phosphorylation of Erk is required for Bad inhibition (Bonni et al., 1999), Bcl-2 activation and neurite growth induced by VPA in SH-SY5Y cells (Yuan et al., 2001). GAP43 is also found to be elevated during neurite formation (Yuan et al., 2001) and is important in growth cone function (Aigner and Caroni, 1993; Biewenga et al., 1996). In the regions we dissected, pErk1/2$^{Thr202/Tyr204}$ and GAP43 were both significantly increased in all three areas exposed to VPA. In addition, 2G13p, a protein found strictly in growth cones (Kim et al., 2011; Maier et al., 2008; Stettler et al., 1999), is increased in periventricular tissue with chronic ICV VPA administration.

Doublecortin (DCX) levels are perturbed if exposure to certain agents alters immature neuron populations (Plane et al., 2008) or if there are asymmetrical distributions of neuroblasts caused by brain tumors (Bexell et al., 2007). We assayed for any abnormal changes in total DCX pools that could suggest tumorigenicity (Bexell et al., 2007) or lowering of immature neuron populations (Umka et al., 2010) but found no difference between samples. Detection of NeuN was used in the same manner, as a known mature neuron marker (Soylemezoglu et al., 2003; Wolf et al., 1996, 1997), and again there was no variance between treatment groups.

Synaptophysin and synaptotagmin are key components of synaptic vesicles (Iwamoto et al., 2004). Assessment of these two proteins was used to look for any increase of synaptic vesicles since our results showed an increase of pErk1/2$^{Thr202/Tyr204}$, 2G13p and GAP43. Our results did not show any change of the total vesicle proteins

after exposure to VPA. These data might reflect stalled growth cones, or possibly that the tissue block size was excessively large, which washed out any small change in synaptic vesicle pools.

Three rats exposed to the highest VPA concentration (3 mM) in this study were not reported due to marked hydrocephaly (data not shown). The dilation of both lateral ventricles produced significant compression of the adjacent tissue making it unusable for tissue imaging and dissection. VPA at 3 mM is notably viscous and various studies that lowered ependymal ciliary movement induced hydrocephalus (Banizs et al., 2005; Del Bigio, 2010; Monkkonen et al., 2007; Nakamura and Sato, 1993; Nyberg-Hansen et al., 1975). In an inherited human disease, primary ciliary dyskinesia (PCD), in which cilia move abnormally or are stationary, leads to an increased likelihood of hydrocephalus (Lee, 2011). It is possible that the inhibition of ciliary movement due to high viscosity of the 3mM VPA led to the enlarged ventricles.

In a manner similar to the work of Pan et al. (2005), who used SH-SY5Y cells to determine neuroprotective dosages of VPA, our whole-animal model allows for the collection of data to help determine biocompatible ICV dosages. Pan et al (2005) included concentrations of 5 mM and 10 mM VPA, however the present study would suggest that these levels could be potentially hazardous for ICV administration (e.g. hydrocephalus).

VPA was localized to the periventricular zone suggesting low tissue penetrance, which may be related to the low concentrations used in the present study. Alternately, a study by the Cornford group (Cornford et al., 1985) demonstrated that in a peripheral administration paradigm, the transport of VPA across the BBB was asymmetrical; the

efflux of brain-to-blood exceeded the influx from blood-to-brain. A study by Shen et al (1992) analyzed cortical resections of patients who had been taking oral valproate and found large variances in plasma-to-brain concentrations (Godin et al., 1969; Shen et al., 1992), noting that cortical levels were significantly lower than unbound/total plasma values; VPA showed the lowest brain-to-blood partitioning of antiepileptic medications (Shen et al., 1992). Patient concentrations of VPA have been reported from 18 μM to 262 μM in cerebrospinal fluid and 39 μM to 185 μM in brain tissue (Vajda et al., 1981). Thus the VPA could have been rapidly carried out of the CNS before deep tissue penetration was obtained. This also suggests that rapid diffusion of VPA from CSF to plasma could recapitulate toxic side effects of oral administration of VPA (e.g. hepatotoxicity; Fisher et al., 1991; Jurima-Romet et al., 1996; Loscher et al., 1984; Sidransky and Verney, 1996).

The present studies coupled with previous work (Serralta et al., 2006) suggest that central administration may be a viable approach to the treatment of intractable seizures. However, some mechanism by which the VPA could be sequestered more effectively in the CNS would be of benefit in such a central administration paradigm. Attempts to retain peripherally administered drugs within the brain have generally used the single or multi-step prodrug approach (Bundgaard, 1989; Stella, 1975). A key concept of the prodrug approach is administration of a non-active form which is metabolized to the active form upon reaching the target site (Bundgaard, 1989). When a prodrug undergoes enzymatic processing, a component of the molecular structure would ensure retention at the site (i.e. brain) (Anderson, 1996; Bodor, 1994; Bodor and Buchwald, 1997). An example of this 'locked-in' approach would be a conjugated phosphate remaining after

metabolism to the active state. Presence of the conjugated phosphate would maintain an anionic charge, thus inhibiting passage back through the BBB and retention within the brain (Somogyi et al., 1998a, 1998b). Since valproic acid has an established efficacy for reducing the incidence of seizures in patients (Chayasirisobhon and Russell, 1983; Gal et al., 1988), applying 'lock-in' concepts to the VPA molecule with ICV administration could produce increased therapeutic potential. While valproic acid has a known ability to help manage intractable seizures (Chayasirisobhon and Russell, 1983; Gal et al., 1988) there is an issue with variability in patient brain and blood plasma levels (Shen et al., 1992) possibly due to the asymmetrical movement of VPA across the blood-brain-barrier (Cornford et al., 1985). Administering VPA intracerebrally in an altered form (i.e. PEGylated) to increase charge and size of the molecule could potentially lead to a more stable and increased level. With this method, a higher concentration within the CSF could possibly be achieved using less drug and yielding significantly decreased blood plasma levels thus reducing the potential for peripheral organ-related side effects (DeWolfe et al., 2009; Fisher et al., 1991; Jurima-Romet et al., 1996; Loscher et al., 1984; Sidransky and Verney, 1996). Thus, there is potential for the use of a centrally administered redesigned VPA molecule to allow for improved seizure control in refractory patients and thus a better quality of life.

CHAPTER V

CONCLUSION

In an animal model, we have shown chronic, centrally administered VPA did not alter behavior, but increased levels of both cell survival phospho-proteins and proteins associated with growth cones. These data suggest that, contrary to the cell death often associated with seizures, central administration of VPA may increase cell survival. The data also suggest that central administration may be a viable route for exploration of efficacy in seizure reduction model to develop this route of administration for potential use in cases of intractable seizures.

REFERENCES

Addis, M.F., Tanca, A., Pagnozzi, D., Crobu, S., Fanciulli, G., Cossu-Rocca, P., Uzzau, S. Generation of high-quality protein extracts from formalin-fixed, paraffin-embedded tissues. Proteom 2009;9:3815-23.

Aigner, L., Caroni, P. Depletion of 43-kDa growth-associated protein in primary sensory neurons leads to diminished formation and spreading of growth cones. J Cell Biol 1993;123: 417-29.

Anderson, B.D. Prodrugs for improved CNS delivery. Adv Drug Del Rev 1996;19:171-202.

Asadi-Pooya, A.A., Sperling, M.R. Clinical features of sudden unexpected death in epilepsy. J Clin Neurophysiol 2009;26:297-301.

Banizs, B., Pike, M.M., Millican, C.L., Ferguson, W.B., Komlosi, P., Sheetz, J., Bell, P.D., Schwiebert, E.M., Yoder, B.K. Dysfunctional cilia lead to altered ependyma and choroid plexus function, and result in the formation of hydrocephalus. Devel 2005;132:5329-39.

Becker, K.F., Mack, H., Schott, C., Hipp, S., Rappl, A., Piontek, G., Hofler, H. Extraction of phosphorylated proteins from formalin-fixed cancer cells and tissues. Open Path J 2008;2:46-52.

Bexell, D., Gunnarsson, S., Nordquist, J., Bengzon, J. Characterization of the subventricular zone neurogenic response to rat malignant brain tumors. Neurosci 2007;147:824-32.

Biewenga, J.E., Schrama, L.H., Gispen, W.H. Presynaptic phosphoprotein B-50/GAP-43 in neuronal and synaptic plasticity. Acta Biochim Pol 1996;43:327-38.

Bodor, N. Drug targeting and retrometabolic drug design approaches introduction. Adv Drug Del Rev 1994;14:157-66.

Bodor, N., Buchwald, P. Drug targeting via retrometabolic approaches. Pharmacol Ther 1997;76:1-27.

Bonni, A., Brunet, A., West, A.E., Datta, S.R., Takasu, M.A., Greenberg, M.E. Cell survival promoted by the Ras-MAPK signaling pathway by transcriptional-dependent and –independent mechanisms. Sci 1999;286:1358-62.

Bundgaard, H. The double prodrug concept and its applications. Adv Drug Del Rev 1989;3:39-65.

Carobrez, A.P., Bertoglio, L.J. Ethological and temporal analysis of anxiety-like behavior: the elevated plus-maze model 20 years on. Neurosci Biobehav Rev 2005;29:1193-205.

Chayasirisobhon, S., Russell, M. Valproic acid and intractable seizures in severely brain-damaged patients. Neurol 1983;33:99-101.

Chin, P.C., Majdzadeh, N., D'Mello, S.R. Inhibition of GSK3beta is a common event in neuroprotection by different survival factors. Mol Brain Res 2005;137:193-201.

Choi, J., Nordli, D.R. Jr., Alden, T.D., DiPatri, A. Jr., Laux, L., Kelley, K., Rosenow, J., Schuele, S.U., Rajaram, V., Koh, S. Cellular injury and neuroinflammation in children with chronic intractable epilepsy. J Neuroinflam 2009;6:1-14.

Cornford, E.M., Diep, C.P., Pardridge, W.M. Blood-brain barrier transport of valproic acid. J Neurochem 1985;44:1541-50.

Cross, D.A., Alessi, D.R., Cohen, P., Andjelkovich, M., Hemmings, BA. Inhibition of glycogen synthase kinase-3 by insulin mediated by protein kinase B Nat 1995;378:785-9.

Cruz, A.P., Frei, F., Graeff, F.G. Ethopharmacological analysis of rat behavior on the elevated plus-maze. Pharmacol Biochem Behav 1994;49:171-6.

Cunningham, M.O., Woodhall, G.L., Jones, R.S. Valproate modifies spontaneous excitation and inhibition at cortical synapses in vitro. Neuropharmacol 2003;45:907-17.

Datta, S.R., Brunet, A., Greenberg, M.E. Cellular survival: a play in three Akts. Genes Dev 1999;13:2905-27.

Del Bigio, M.R. Ependymal cells: biology and pathology. Acta Neuropathol 2010;119:55-73.

DeWolfe, J.L., Knowlton, R.C., Beasley, M.T., Cofield, S., Faught, E., Limdi, N.A. Hyperammonemia following intravenous valproate loading. Epil Res 2009;85:65-71.

Di Daniel, E., Mudge, A.W., Maycox, P.R. Comparative analysis of the effects of four mood stabilizers in SH-SY5Y cells and in primary neurons. Bipol Disord 2005;7:33-41.

Doremus, T.L., Varlinskaya, E.I., Spear, L.P. Factor analysis of elevated plus-maze behavior in adolescent and adult rats. Pharmacol Biochem Behav 2006;83:570-7.

Einat, H., Yuan, P., Gould, T.D., Li, J., Du, J., Zhang, L., Manji, H.K., Chen, G. The role of the extracellular signal-regulated kinase signaling pathway in mood modulation. J Neurosci 2003;23:7311-6.

Ennaceur, A., Michalikova, S., Chazot, P.L. Models of anxiety: responses of rats to novelty in an open space and enclosed space. Behav Brain Res 2006;171:26-49.

Ennaceur, A., Michalikova, S., van Rensburg, R., Chazot, P.L. Models of anxiety: responses of mice to novelty and open spaces in a 3D maze. Behav Brain Res 2006;174:9-38.

Faratian, D., Um, I.H., Wilson, D.S., Mullen, P., Langdon, S.P., Harrison, D.J. Phosphoprotein pathway profiling of ovarian carcinoma for the identification of potential new targets for therapy. Euro J Canc 2011;47:1420-31.

Faught, E., Morris, G., Jacobson, M., French, J., Harden, C., Montouris, G., Rosenfeld, W. Adding lamotrigine to valproate: incidence of rash and other adverse effects. Epilepsia 1999;40:1135-40.

Fisher, R., Nau, H., Gandolfi, A.J., Brendel, K. Toxicity of valproic acid in liver slices from sprague-dawley rats and domestic pigs. Toxicol in Vitro 1991;5:201-5.

Gal, P., Oles, K.S., Gilman, J.T., Weaver, R. Valproic acid efficacy, toxicity, and pharmacokinetics in neonates with intractable seizures. Neurol 1988;38:467-71.

Godin, Y., Heiner, L., Mark, J., Mandel, P. Effects of DI-n-propylacetate, and anticonvulsive compound, on GABA metabolism. J Neurochem 1969;16:869-73.

Goren, I., Muller, E., Pfeilschifter, J., Frank, S. Thr308 determines Akt1 nuclear localization in insulin-stimulated keratinocytes. Biochem Biophys Res Com 2008;372:103-7.

Grimes, C.A., Jope, R.S. The multifaceted roles of glycogen synthase kinase 3beta in cellular signaling. Prog Neurobiol 2001;65:391-426.

Hassan, M.N., Laljee, H.C.K., Parsonage, M.J. Sodium valproate in the treatment of resistant epilepsy. Acta Neuro Scand 1976;54:209-18.

Higuchi, T., Yamazaki, O., Takazawa, A., Kato, N., Watanabe, N., Minatogawa, Y., Tamazaki, J., Ohshima, H., Nagaki, S., Igarashi, Y. Effects of carbamazepine and valproic acid on brain immunoreactive somatostatin and gamma-aminobutyric acid in amygdaloid-kindled rats. Eur J Pharmacol 1986;125:169-75.

Hitiris, N., Mohanrai, R., Norrie, J., Brodie, M.J. Mortality in epilepsy. Epil Behav 2007;10:363-76.

Iwamoto, M., Hagishita, T., Shoji-Kasai, Y., Ando, S., Tanaka, Y. Age-related changes in the levels of voltage-dependent calcium channels and other synaptic proteins in rat brain cortices. Neurosci Lett 2004;19:277-81.

Jurima-Romet, M., Abbott, F.S., Tang, W., Huang, H.S., Whitehouse, L.W. Cytotoxicity of unsaturated metabolites of valproic acid and protection by vitamins C and E in glutathione-dependent rat hepatocytes. Toxicol 1996;112:69-85.

Kandel, E.S., Hay, N. The regulation and activities of the multifunctional serine/threonine kinase Akt/PKB. Exp Cell Res 1999;253:210-29.

Khor, T.O., Gul, Y.A., Ithnin, H., Seow, H.F. Positive correlation between overexpression of phospho-BAD with phosphorylated Akt at serine 473 but not threonine 308 in colorectal carcinoma. Canc Lett 2004;210:139-50.

Kim, S.R., Chen, X., Oo, T.F., Kareva, T., Yarygina, O., Wang, C., During, M., Kholodilov, N., Burke, R.E. Dopaminergic pathway reconstruction by Akt/Rheb-induced axon regeneration. Ann Neurol 2011;70:110-20.

Kitagawa, K., Takasawa, K., Kuwabara, K., Sasaki, T., Tanaka, S., Mabuchi, T., Sugiura, S., Omura-Matsuoka, E., Matsumoto, M., Hori, M. Differential Akt phosphorylation at Ser473 and Thr308 in cultured neurons after exposure to glutamate in rats. Neurosci Lett 2002;333:187-90.

Kumari, S., Liu, X., Nguyen, T., Zhang, X., D'Mello, S.R. Distinct phosphorylation patterns underlie Akt activation by different survival factors in neurons. Mol Brain Res 2001;96:157-62.

Lamarre, M., Desrosiers, R.R. Up-regulation of protein L-isoaspartyl methyltransferase expression by lithium is mediated by glycogen synthase kinase-3 inactivation and beta-catenin stabilization. Neuropharmacol 2008;55:669-79.

Lee, L. Mechanisms of mammalian ciliary motility: insights from primary ciliary dyskinesia genetics. Gene 2011;473:57-66.

Lipkind, D., Sakov, A., Kafkafi, N., Elmer, G.I., Benjamini, Y., Golani, I. New replicable anxiety-related measures of wall vs center behavior of mice in the open field. J Appl Physiol 2004;97:347-59.

Loscher, W. Correlation between alteration in brain GABA metabolism and seizure excitability following administration of GABA aminotransferase inhibitors and valproic acid – a re-evaluation. Neurochem Int 1981;3:397-404.

Loscher, W. Valproate: a reappraisal of its pharmacodynamics properties and mechanisms of action. Prog Neurobiol 1999;58:31-59.

Loscher, W., Nau, H., Marescaux, C., Vergnes, M. Comparative evaluation of anticonvulsant and toxic potencies of valproic acid and 2-en-valproic acid in different animal models of epilepsy. Eur J Pharmacol 1984;99:211-8.

Maier, I.C., Baumann, K., Thallmair, M., Weinmann, O., Scholl, J., Schwab, M.E. Constraint-induced movement therapy in the adult rat after unilateral corticospinal tract injury. J Neurosci 2008;28:9386-403.

Monkkonen, K.S., Hakumaki, J.M., Hirst, R.A., Miettinen, R.A., O'Callaghan, C., Mannisto, P.T., Laitinen, J.T. Intracerebroventricular antisense knockdown of G alpha i2 results in ciliary stasis and ventricular dilation in the rat. BMC Neurosci 2007;8:1-15.

Nakamura, Y., Sato, K. Role of disturbance of ependymal ciliary movement in development of hydrocephalus in rats. Chil Nerv Sys 1993;9:65-71.

Nobili, L., Proserpio, P., Rubboli, G., Montano, N., Didato, G., Tassinari, C.A. Sudden unexpected death in epilepsy (SUDEP) and sleep. Sle Med Rev 2010;15:237-46.

Nutt, J.G., Burchiel, K.J., Comella, C.L., Jankovic, J., Lang, A.E., Laws, E.R. Jr., Lozano, A.M., Penn, R.D., Simpson, R.K. Jr., Stacy, M., Wooten, G.F. Randomized, double-blind trial of glial cell line-derived neurotrophic factor (GNDF) in PD. Neurol 2003;60:69-73.

Nyberg-Hansen, R., Torvik, A., Bhatia, R. On the pathology of experimental hydrocephalus. Neurobiol 1975;95:343-50.

Obara, D., Utsugisawa, K., Nagane, Y., Tohgi, H. Hypoxic condition interferes with phosphorylation of Akt at Thr(308) in cultured rat pheochromocytoma-12 cells. Neurosci Lett 2002;332:167-70.

Ouyang, Y.B., Zhang, X.H., He, Q.P., Wang, G.X., Siesjo, B.K., Hu, B.R. Differential phosphorylation at Ser473 and Thr308 of Akt-1 in rat brain following hypoglycemic coma. Brain Res 2000;876:191-5.

Pan, T., Li, X., Xie, W., Jankovic, J., Le, W. Valproic acid-mediated Hsp70 induction and anti-apoptotic neuroprotection in SH-SY5Y cells. FEBS Lett 2005;579:16-20.

Paxinos, G., Watson, C. The rat brain: in stereotaxic coordinates. 2nd ed. San Diego, California;1997.

Pellow, S., Chopin, P., File, S.E., Briley, M. Validation of open: closed arm entries in an elevated plus-maze as a measure of anxiety in the rat. J Neurosci Meth 1985;14:149-67.

Plane, J.M., Whitney, J.T., Schallert, T., Parent, J.M. Retinoic acid and environmental enrichment alter subventricular zone and striatal neurogenesis after stroke. Exp Neurol 2008;214:125-34.

Prut, L., Belzung, C. The open field as a paradigm to measure the effects of drugs on anxiety-like behaviors: a review. Eur J Pharmacol 2003;463:3-33.

Redenbaugh, J.E., Sato, S., Penry, J.K., Dreifuss, F.E., Kupferberg, H.J. Sodium valproate: pharmacokinetics and effectiveness in treating intractable seizures. Neurol 1980;30:1-6.

Salvatore, M.F., Ai, Y., Fischer, B., Zhang, A.M., Grondin, R.C., Zhang, Z., Gerhardt, G.A., Gash, D.M. Point source concentration of GDNF may explain failure of phase II clinical trial. Exp Neurol 2006;202:497-505.

Schechter, P.J., Tranier, Y., Grove, J. Effect of n-dipropylacetate on amino acid concentrations in mouse brain: correlations with anti-convulsant activity. J Neurochem 1978;31:1325-7.

Scheid, M.P., Woodgett, J.R. PKB/AKT: functional insights from genetic models. Nat Rev Mol Cell Biol 2001;2:760-8.

Serralta, A., Barcia, J.A., Ortiz, P., Duran, C., Hernandez, M.E., Alos, M. Effect of intracerebroventricular continuous infusion of valproic acid versus singel i.p. and i.c.v. injections in the amygdala kindling epilepsy model. Epilepsy Res 2006;70:15-26.

Shen, D.D., Ojemann, G.A., Rapport, R.L., Dills, R.L., Friel, P.N., Levy, R.H. Low and variable presence of valproic acid in human brain. Neurol 1992;42:582-5.

Shi, S.R., Liu, C., Balgley, B.M., Lee, C., Taylor, C.R. Protein extraction from formalin-fixed, paraffin-embedded tissue sections: quality evaluation by mass spectrometry. J Histochem Cytochem 2006;54:739-43.

Sidransky, H., Verney, E. Toxic effect of valproic acid on tryptophan binding to rat hepatic nuclei. Toxicol 1996;109:39-47.

Simler, S., Ciesielski, L., Maitre, M., Randrianarisoa, H., Mandel, P. Effect of sodium n-dipropylacetate on audiogenic seizures and brain gamma-aminobutyric acid level. Biochem Pharmacol 1973;22:1701-8.

Somogyi, G., Buchwald, P., Nomi, D., Prokai, L., Bodor, N. Targeted drug delivery to the brain via phosphonate derviatives II. anionic chemical delivery system for azidovudine (AZT). Int J Pharma 1998;166:27-35.

Somogyi, G., Nishitani, S., Nomi, D., Buchwald, P., Prokai, L., Bodor, N. Targeted drug delivery to the brain via phosphonate derivatives: I. design, synthesis and evaluation of an anionic chemical delivery system for testosterone. Int J Pharma 1998;166:15-26.

Soylemezoglu, F., Onder, S., Tezel, G.G., Berker, M. Neuronal nuclear antigen (NeuN): a new tool in the diagnosis of central neurocytoma. Pathol Res Pract 2003;199:463-8.

Stanford, S.C. The open field test: reinventing the wheel. J Psychopharmacol 2007;21:134-5.

Stella, V. Pro-drugs as Novel Drug Delivery Systems. ACS Symp Ser 1975;14:1-115.

Stettler, O., Bush, M.S., Kasper, M., Schlosshauer, B., Gordon-Weeks, P.R. Monoclonal antibody 2G13, a new axonal growth cone marker. J Neurocytol 1999;28:1035-44.

True, L. Quality control in molecular immunohistochemistry. Histochem Cell Biol 2008;130:473-80.

Umka, J., Mustafa, S., ElBeltagy, M., Thorpe, A., Latif, L., Bennett, G., Wigmore, P.M. Valproic acid reduces spatial working memory and cell proliferation in the hippocampus. Neurosci 2010;166:15-22.

Vajda, F.J.E., Donnan, G.A., Phillips, J., Bladin, P.F. Human brain, plasma, and cerebrospinal fluid concentration of sodium valproate after 72 hours of therapy. Neurol 1981;31:486-7.

Velling, T., Stefansson, A., Johansson, S. EGFR and beta1 integrins utilize different signaling pathways to activate Akt. Exp Cell Res 2008;314:309-16.

Vreugdenhil, M., van Veelen, C.W., van Rijen, P.C., Lopes da Silva, F.H., Wadman, W.J. Effects of valproic acid on sodium currents in cortical neurons from patients with pharmaco-resistant temporal lobe epilepsy. Epil Res 1998;32:309-20.

Wasterlain, C.G., Shirasaka, Y. Seizures, brain damage and brain development. Brain Dev 1994;16:279-95.

Wolf, H.K., Buslei, R., Blumcke, I., Wiestler, O.D., Pietsch, T. Neural antigens in oligodendrogliomas and dysembryoplastic neuroepithelial tumors. Acta Neuropathol 1997;94:436-43.

Wolf, H.K., Buslei, R., Schmidt-Kastner, R., Schmidt-Kastner, P.K., Pietsch, T., Wiestler, O.D., Blumcke, I. NeuN: a useful neuronal marker for diagnostic histopathology. J Histochem Cytochem 1996;44:1167-71.

Yuan, P.X., Huang, L.D., Jiang, Y.M., Gutkind, J.S., Manji, H.K., Chen, G. The mood stabilizer valproic acid activates mitogen-activated protein kinases and promotes neurite growth. J Biol Chem 2001;276:31674-83.

Zhang, X.Z., Li, X.J., Zhang, H.Y. Valproic acid as a promising agent to combat Alzheimer's disease. Brain Res Bul 2010;81:3-6.